JCTC Journal of Chemical Theory and Computation

pubs.acs.org/JCTC Article

A Method for Obtaining Liquid−Solid Adsorption Rates from Molecular Dynamics Simulations: Applied to Methanol on Pt(111) in H_2O

Xiaohong Zhang, Aditya Savara,* and Rachel B. Getman*

Cite This: J. Chem. Theory Comput. 2020, 16, 2680−2691 Read Online

ACCESS | Metrics & More | Article Recommendations | Supporting Information

ABSTRACT: Adsorption is an important step in heterogeneous catalysis as it predetermines how many reactant molecules can participate in a surface reaction per unit time. While the rate of adsorption processes is well studied in gas−solid adsorption in both theory and experiment, such rates are still not well studied for liquid−solid adsorption. This is partly because the ever-changing configurations of liquid-phase solvent molecules impede the ability to study a molecule approaching a surface from a liquid phase by either experiment or theory. In this work, we develop a method using molecular dynamics (MD) simulations to study the rate of adsorption in liquid−solid adsorption processes. Specifically, we use MD to model the diffusion of a methanol molecule in aqueous solvent and its adsorption to a Pt(111) surface. We find that by approximating the solute motion as following the same displacement rates as a random walk model, the adsorbed and non-adsorbed states of the methanol molecule near the Pt(111) surface can be discerned and quantified. In particular, this methodology enables extracting a sticking coefficient and a macroscopically relatable adsorption rate. This method can be applied to arbitrary types of reactants and surfaces, as well as different liquid environments, thus providing a general tool for predicting quantitative adsorption rates of liquid−solid adsorption systems.

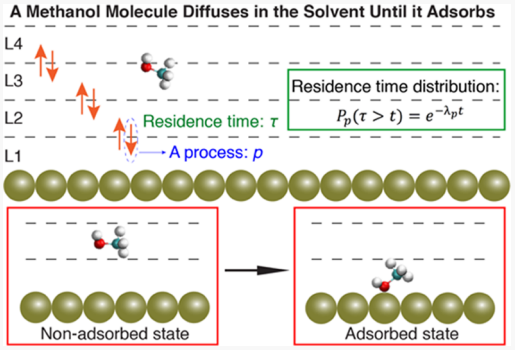

1. INTRODUCTION

Aqueous-phase heterogeneous catalysis has many applications, including biomass reforming, Fischer−Tropsch synthesis, and electrocatalysis.[1,2] Formulation of accurate kinetic models for these systems is necessary not only to gain mechanistic understanding but also to have quantitative prediction of the activity and selectivity under reaction conditions.[3] Many studies on aqueous-phase catalysis have found that the liquid solvation environment can influence the reaction mechanisms and kinetics differently than the gas phase, e.g., by forming hydrogen bonds with reaction intermediates, co-catalyzing certain reactions, and affecting kinetic barriers and reaction mechanisms.[4−7] However, most of the studies on aqueous-phase catalysis focus on surface intermediate reaction steps; whereas, for a full catalytic cycle, the kinetics of adsorption from the liquid solvation environment to the surface are equally important.[8] Despite its importance, understanding how the aqueous environment influences adsorption kinetics in aqueous-phase heterogeneous catalysis is significantly less developed.

In the adsorption process, species from the fluid phase (gas or liquid) are localized at the surface. The adsorption rate per unit area σ is usually written as

$$r_{\mathrm{ads},\sigma} = F \times S \times \theta_S \quad (1)$$

where F is the flux, S is the sticking coefficient (i.e., the fraction of impinging molecules that stick to the surface), and θ_S is the number of surface sites per unit surface area that is available for adsorption. Sticking can occur either directly when the molecule encounters the surface or via *trapping*, which involves the molecule binding transiently to the surface, resulting in a short-lived adsorbed state that can serve as a precursor to sticking. At the mesoscopic system level, F depends on three factors external to the elementary reaction step:[9−11] (1) the rate of diffusion of the fluid molecule from the bulk fluid phase to the solid surface, (2) the concentration of the fluid molecule in the gas or liquid phase, and (3) the functional form for the flux, i.e., the rate of collisions/encounters that result in an average number of opportunities for adsorption per unit time. In gas−solid adsorption, the flux is calculated from collision theory as[9,11,12]

Received: December 16, 2019
Published: March 5, 2020

https://dx.doi.org/10.1021/acs.jctc.9b01249
J. Chem. Theory Comput. 2020, 16, 2680−2691

$$F_{g-s} = \frac{P_A}{\sqrt{2\pi m k_B T}} \quad (2)$$

where P_A is the partial pressure of the adsorbing species, m is its molecular mass, k_B is Boltzmann's constant, and T is the temperature. Theoretical calculations of the sticking coefficient are not trivial, partly due to challenges in calculating the steric factor, which determines the fraction of orientations of the fluid molecule relative to the surface that are capable of sticking.[13−19] In gas−solid adsorption, every *encounter* between a gas molecule and the solid surface results in a single *collision* event, which enables quantification of the sticking coefficient using experimental[20−24] or empirical[25,26] methods. In liquid−solid adsorption, the number of encounters does not equal the number of collisions. In contrast to gas−solid adsorption, the impinging molecules undergo multiple collisions per encounter, which makes it more challenging to determine the flux and sticking coefficient. The difference between an encounter and a collision is depicted in Figure 1; these terms and others, which

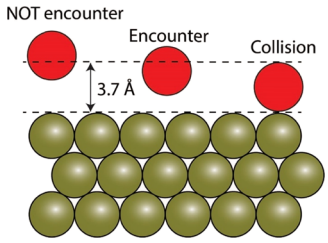

Figure 1. Molecule (red sphere) approaches (left), encounters (middle), and collides with (right) a Pt(111) surface (gold spheres). These different events are distinguished by the distance of the molecule from the surface relative to the diameter of the molecule (in this work: 3.7 Å for methanol).

are italicized on first mention, are collected in a table of terms and definitions in an Appendix. Even with this challenge, a handful of experimental studies have measured sticking frequencies or sticking coefficients indirectly with the use of physically realistic models and numerical simulations or approximations.[10,12,27−30] However, these studies are limited to specific systems and, in most cases, require specialized analytical techniques. A general strategy for predicting and assessing sticking phenomena in the liquid phase is still an outstanding problem.

Molecular dynamics (MD) simulations are practical for sampling the diverse environments that liquid molecules experience[31] and for developing general strategies to obtain liquid−solid sticking coefficients. In this work, we present a method based on MD simulations to calculate the *encounter sticking coefficient* (S_E), which is the probability per encounter that a molecule ultimately sticks to the solid surface. To apply this method, MD is first used to simulate the diffusion of a methanol molecule in an aqueous solvent and its adsorption to and desorption from a Pt(111) surface, with multiple encounters occurring per simulation. Motions of the methanol molecule normal to the surface are approximated as having the same rate of motion as a continuous time random walk (CTRW). The data from each simulation is fitted with a Poisson distribution of the residence times within fluid *layers* above the catalyst surface, which is used to extract S_E. Using this treatment, we find that the average lifetimes of adsorbed versus non-adsorbed states of the methanol molecule near the Pt(111) surface can be separated and quantified, providing a straightforward tool for studying the adsorption rate and obtaining parameters needed in microkinetic modeling.

2. THEORY

Extraction of the liquid−solid sticking coefficient is non-trivial even in molecular simulations, in part due to the challenge of separating collisions from encounters. An encounter is the time when the potentially adsorbing molecule is in the fluid phase neighboring the surface; whereas, a collision occurs when the distance between the molecule and the surface equals the sum of the radii of the molecule and a surface atom (Figure 1). In a liquid phase, each encounter consists of many collisions, and each collision may or may not result in sticking. Even encounters that consist of many thousands of collisions may not result in sticking since the process of sticking may be activated. In addition to the possibility of an activation energy, impinging molecules can experience a variety of configurations during an encounter, which makes it challenging to determine the encounter sticking coefficient S_E. An intuitive idea for extracting S_E from MD simulations is to use molecular coordinates, but such an approach is complicated for two reasons: (1) molecules can adsorb in multiple types of surface sites (e.g., atop and bridge) and adsorption geometries (e.g., due to intramolecular rotations), which are difficult to predict ahead of time and (2) molecules that have encountered the surface but not undergone sticking can assume geometries that resemble those of an adsorbed molecule. Even when geometric criteria can be used to determine when a molecule has adsorbed to the surface, that knowledge alone would still be insufficient to calculate the sticking coefficient since calculation of the sticking coefficient also requires extracting the number of encounters. Consequently, while geometric algorithms are useful, they are complementary to rather than a replacement for the methodology introduced herein. In this work, we describe a method that is based on tracking the motions of the molecule perpendicular to the surface generated in atomistic MD simulations and fitting the resulting distributions of times that the molecule spends at different distances from the surface. Since this approach utilizes atomistic simulations, it captures the diverse set of configurations that the molecule can sample. This approach is also compatible with situations where the accessible adsorption states are not known before the simulation.

In this study, we calculate S_E for a methanol molecule on a Pt(111) surface under the aqueous phase. We know from density functional theory (DFT) analysis that methanol prefers to bind to Pt(111) via its oxygen atom.[5] Hence, we track the motions of the oxygen atom normal to the surface in our MD simulations, and we use these to determine encounters for quantification of S_E. Specifically, the MD simulation box is divided into layers (Figure 2) with heights equal to the diameter of the methanol molecule. The diameter of the methanol molecule is determined using DFT calculations. Briefly, we calculate the interaction energy between the methanol molecule and the Pt surface as a function of distance from the surface and plot the results. The distance at which the interaction energy goes to 20% of the full interaction is taken as the methanol diameter. Full details of this analysis are provided in the Supporting Information Section S1. To calculate S_E, we take continuous position data for the methanol molecule relative to the Pt(111) surface and bin it into different fluid layers. This enables us to determine the amount

https://dx.doi.org/10.1021/acs.jctc.9b01249
J. Chem. Theory Comput. 2020, 16, 2680−2691

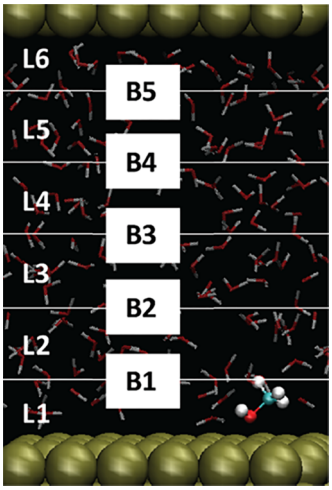

Figure 2. Periodic simulation box used in this work comprising an aqueous-phase methanol molecule and a Pt(111) surface. The fluid is broken into layers (L), which are separated by boundary planes (B). Water molecules are de-emphasized for clarity. The distance between periodic Pt(111) surfaces (i.e., from the top of the lower surface to the bottom of the upper surface in the next adjacent image) is 21.3629 Å, and each layer is 3.7 Å thick except for L6 (See Section 2.1). Color key: C = cyan, H = white, O = red, and Pt = gold.

of time that the molecule spends in fluid layers at different distances from the Pt(111) surface. The amount of time spent in a layer is the residence time for that layer. To determine the residence times for the different layers, we track the number of times that the molecule "hops" between layers. The word "hop" here has a meaning that is different from typical surface kinetics studies. In surface kinetics, a hop typically means that the molecule has moved from one stable (or metastable) binding site to another, e.g., moving between adjacent sites in a lattice; whereas in this work, a hop refers to the molecule diffusing across a geometric *boundary* (i.e., analogous to a walk step in random walk model). We note that boundaries and layers are separate terms; layers are volumes, and boundaries are planes that separate layers (these terms are not related to the "boundary layers" in continuum fluid dynamics). In contrast to surface kinetics studies, hops in this work do not necessarily correspond to crossing an activation barrier. In this work, we assume that hops can be coarse grained as a continuous time random walk (CTRW) with a fixed step length. This enables us to use the distribution of residence times that the methanol molecule spends in particular layers (which are the durations of individual encounters[10]) as indication of how quickly molecules exchange positions with their neighbors in a particular direction. Fitting this distribution of times allows extraction of S_E. The assumptions made in this work are as follows.

2.1. Vertical Motions of a Solvated Molecule Can Be Described by a Continuous-Time Random-Walk (CTRW) Model. We chose this model based on the assumption that methanol diffusion around water molecules obeys a first-order Fickian mechanism,[12,27,30,32] consistent with molecular transport and a random walk process.[33] Then, the motions of the methanol molecule can be simplified as hops between fluid layers perpendicular to the Pt(111) surface. Layers are labeled L1−L6 and have corresponding boundary planes labeled B1−B5 in Figure 2. In our model, L1 is referred to as the "adjacent layer" because it is adjacent to the Pt(111) surface. While L6 is also adjacent to Pt(111), it does not constitute a "full" layer due to differences in the sizes of the solvent and solute molecules (see the Supporting Information), and hence, all references to "the Pt surface" or "the surface" are to the lower Pt surface in Figure 2. Furthermore, since we only study the lower Pt surface with the adjacent layer and enough layers to represent the "bulk" solvent, we only report information for L1−L4 in this manuscript. The hop length (functioning as a random walk step length) between neighboring layers is fixed and equal to the layer length, which is defined here as a methanol kinetic diameter of 3.7 Å. How this value influences the results is discussed in the Supporting Information Section S6. Herein, we define hops moving toward the surface as "forward" hops and hops moving away from the surface as "reverse" hops.

2.2. The Residence Time (τ) that a Molecule Stays in a Particular Layer Can be Modeled with a Poisson Distribution. Suppose a methanol molecule enters a layer at time $t = 0$, the residence time is then the amount of time that the methanol molecule stays in this layer until time t ($t > 0$) when it hops to another layer. This is called a *visit*. During MD simulation, the methanol molecule hops between layers multiple times, and for each individual hop, there is an associated residence time. The total residence time in each layer is modeled using a Poisson distribution (the relevant expressions are provided in eqs 3, 4, and 6). Since the presence of the Pt(111) surface provides asymmetry and causes anisotropic motions of the methanol molecule, we track residence times in both the forward and reverse directions. This accounting is indicated by subscripting τ. For example, $\tau_{B1F,T}$ denotes the average residence time that the molecule spends in L2 before it crosses boundary B1, i.e., before it hops in the forward direction (F) to L1. The T in the subscript stands for "total" to indicate that $\tau_{B1F,T}$ corresponds to a sum over all forward processes across B1. Considering L2, for example, a molecule in L2 could hop either to L1 or to L3. $\tau_{B1F,T}$ is the total time that the molecule spends in L2 before hopping to L1. $\tau_{B1F,T}$ is thus less than the total residence time for L2. For example, if the molecule stays in L2 for a total of 100 ps where 45 of the 100 ps results in the molecule hopping to L1 (hence, 55 ps results in hopping to L3) then $\tau_{B1F,T} = 45$ ps.

2.3. The Diverse States that the Solvated Molecule Accesses Can Be Lumped into a Small Number of Kinetically Distinct Sets of States within Each Layer. Within the solvent layers, there can be multiple states (thousands or more) arising from the multiple conformations that the molecule can access, multiple configurations that the solvent can take on, and multiple types of interactions at play between the molecule and the solvent (e.g., via hydrogen bonding). We assume that these diverse states can be chemically lumped into kinetically distinct *sets of states (SoS)* and that the number of SoS is smaller, to the extent of being countable. For example, it may be that all conformations of methanol that form a specific number (n_{HB}) of hydrogen bonds with the surrounding water environment could be lumped into a single SoS, regardless of the configurations of the surrounding water molecules. It is not necessary to know the chemical origins of the different SoS to apply the method presented here; in fact, the method presented here can be used to gain chemical information about the different SoS without any prior knowledge. The different SoS give rise to kinetically distinct diffusion/desorption rates, with diffusion/desorption

https://dx.doi.org/10.1021/acs.jctc.9b01249
J. Chem. Theory Comput. 2020, 16, 2680−2691

being faster for some SoS (short-lived states) and slower for other SoS (long-lived states). For example, for L1, we anticipate at least two types of SoS, including at least one adsorbed SoS (long-lived state) and at least one non-adsorbed SoS (short-lived state). Depictions of adsorbed (i.e., through the oxygen atom) and non-adsorbed states in L1 are shown in Figure 3. Each SoS has its own characteristic residence time,

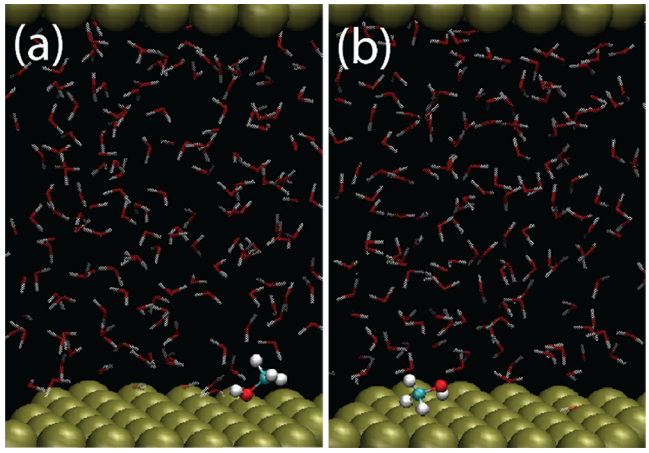

Figure 3. Methanol encountering the Pt surface in (a) an adsorbed state (long residence time), and (b) a non-adsorbed state (short residence time).

which can be modeled with a Poisson distribution.[34,35] Specifically, the Poisson distribution is used to model the probability per unit time that the methanol molecule transitions between one SoS to another.

2.4. Each Kinetically Distinct Type of Transition Is a *Process* (*p*) with Transition Frequencies that Can Be Modeled Using a Poisson Distribution. These processes move the solute between SoS, with each such movement being a transition event. For example, moving from a particular SoS in L2 to a particular SoS in L3 is a process; each time this happens is a transition event. When modeled by a Poisson distribution, the probability of a process event occurring within a particular unit time is expected to obey the probability density function

$$P_{\mathrm{p}}(n,\, t) = \frac{(\lambda_{\mathrm{p}} t)^n}{n!} \mathrm{e}^{-\lambda_{\mathrm{p}} t} \tag{3}$$

where n represents the specific number of hop events to have occurred within time t and λ_{p} is the average transition frequency (hopping rate) for that process. We anticipate that there will be at least two processes associated with hopping from L1 to L2, one due to desorption and one due to diffusion. When methanol has a long lifetime in L1, it will on average be due to an adsorbed SoS produced by sticking. In contrast, for hopping between other layers (where there is no surface), the hopping rate between layers is solely due to diffusion, though there still may be more than one SoS and thus more than one diffusion process. To extract information about the statistics of the SoS, we must consider the distribution for the number of visits (V) that have residence times longer than some time t within a given layer. This information can be modeled using a *raw survival distribution function* (RSDF), i.e., an unscaled complementary cumulative distribution function of eq 3 that represents the probability that the molecule resides in a state beyond a certain length of time

$$P_{\mathrm{p}}(\tau > t) = \mathrm{e}^{-\lambda_{\mathrm{p}} t} \tag{4}$$

where $P_{\mathrm{p}}(\tau > t)$ is the probability of occurrence for a particular residence time $\tau > t$. Equation 4 enables us to resolve the statistics for processes from a given SoS that are associated with different diffusion/desorption rates. Resolving the extent of non-adsorbed versus adsorbed SoS in L1 is essential to extract the effective S_{E}, as it enables us to distinguish the percentage of visits that result in adsorption.

$$S_{\mathrm{E}} = \frac{V_{\mathrm{B1F,A}}}{V_{\mathrm{B1F,T}}} \tag{5}$$

where the subscript A stands for the adsorbed (and the subscript B1F indicates the total forward visits across B1, i.e., into adsorbed and non-adsorbed SoS).

The process flow for the procedure presented in this work is provided in Figure 4. The innovative aspect is to extract $V_{\mathrm{B1F,\,A}}$

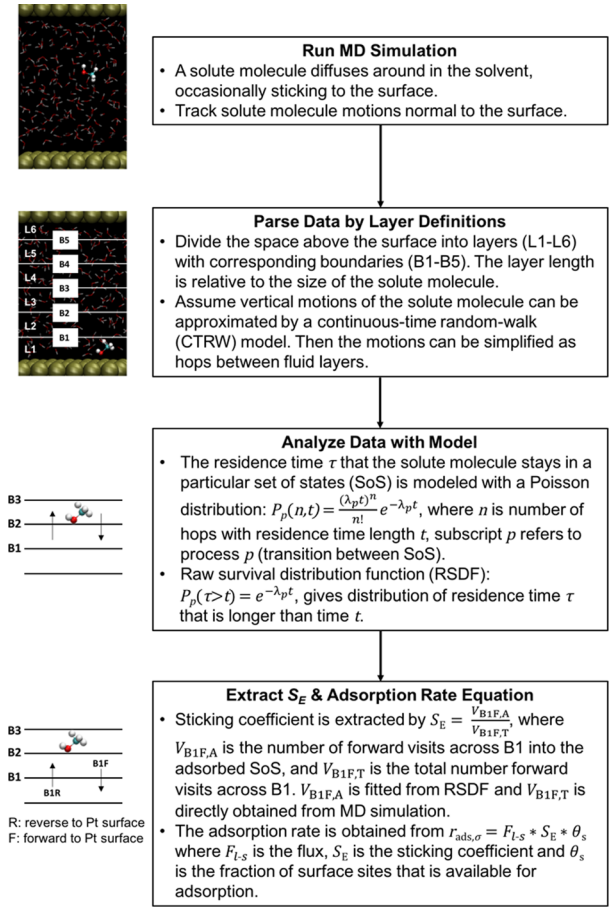

Figure 4. Process flow used in this work to obtain the sticking coefficient S_{E} and adsorption rate equation. Feedback loops are not required provided that appropriate boundaries have already been chosen and the run time is sufficiently long.

(and V_{B1F}) from MD simulations by analyzing the distribution of visit residence times within the different layers. We carry out such an analysis for MD simulations of the methanol/water/Pt(111) system in Section 4.

3. SIMULATION METHODS

3.1. System Setup. The Pt surface is modeled with a three-layer thick 6 Pt × 6 Pt slab in a periodic supercell with *a*

https://dx.doi.org/10.1021/acs.jctc.9b01249
J. Chem. Theory Comput. 2020, 16, 2680−2691

= 16.8318 Å, b = 14.5768 Å, and c = 28.6979 Å. The c dimension is determined using MD in the NPT ensemble to attain the proper density of bulk H_2O (of 1 g/cm^3 in the middle of the unit cell).[6,36] The full procedure for obtaining this value is discussed in detail in our prior work.[6,36] The simulation box comprises one methanol molecule and 165 H_2O molecules above the Pt(111) surface. The size of the unit cell (and hence the number of H_2O molecules) is chosen to balance computational expense with the requirement of having two types of H_2O in the system: interfacial H_2O (near the surface) and bulk H_2O (further from the surface). This unit cell size is suitable to have one methanol molecule in the system, which simplifies the analysis of methanol diffusion, while maintaining a reasonable methanol concentration (of 0.32 mol/L). We have previously tested the effect of varying the number of H_2O molecules on the water structure at a Pt(111) interface[6] and found that interfacial properties are constant when between 24 and 240 H_2O molecules are used in the MD simulation. Results of these tests are provided in Section S4 of the Supporting Information. Based on these results, we do not expect the small size of the unit cell to influence the interfacial behavior of the methanol molecule in our simulations.

3.2. Molecular Dynamics Simulation. MD simulations are carried out using the large-scale atomic/molecular massively parallel simulator (LAMMPS), similar to our prior work.[6,36] Intermolecular energies in LAMMPS are calculated using pairwise Lennard-Jones + Coulomb (LJ + C) potentials. LJ interactions are calculated up to cutoff distances of 10 Å. This distance is chosen since all LJ interactions are ∼0 at this distance. Water molecules are modeled using the flexible transferable intermolecular potential with 3 points−Chemistry at Harvard Macromolecular Mechanics (TIP3P/CHARMM)[37]force field, the methanol molecule is modeled using the optimized potentials for liquid simulations (OPLS-AA)[38] force field, and Pt atoms are modeled using the universal force field (UFF),[39] with the exception that the partial charges on the Pt atoms are set to 0 in our models. The positions of all Pt atoms are held fixed during all simulations. All LJ cross terms are calculated with geometric mixing rules, except for the intermolecular O−H interactions between H_2O molecules, which employ Lorentz−Berthelot mixing rules. The particle−particle particle−mesh (PPPM) method is used to calculate long-range Coulomb interactions to an accuracy of 10^{-4}. All LJ + C model parameters are provided in the Supporting Information. Following simulation box initialization (described in detail in our prior work[6,36]), diffusion of the methanol molecule in liquid H_2O solvent is simulated in the canonical (NVT) ensemble at 300 K, which is maintained with a Nosé−Hoover thermostat. The NVT simulation is carried out for a total of 200 ns using 1 fs timesteps. The first 2 ns are used for system equilibration, and the remaining time is the production run. The positions of the methanol O atom are sampled every 10 fs during the production runs. A total of 10 NVT simulations are performed. Results reported herein are averages over those 10 simulations unless specified otherwise. For averaged quantities, two standard deviations are used for the 95% confidence intervals.

4. RESULTS

According to the development in Section 2, two quantities are needed in order to calculate S_E: $V_{B1F,T}$ and $V_{B1F,A}$. We discuss how we obtain $V_{B1F,T}$ in Section 4.1 and how we extract $V_{B1F,A}$ in Section 4.2. Then, in Section 4.3, we use these quantities to calculate an apparent rate constant for adsorption, which is needed in conventional kinetic modeling. These values are expected to depend on the simulation temperature; all values presented herein were obtained using a simulation temperature of 300 K.

4.1. Methanol Hopping between Layers. Figure 5 plots the number of times the methanol molecule hops across B1−B3 in both the forward and reverse directions during our MD simulations. We are especially interested in the number of forward hops across boundary B1, as this quantity is equal to the total number of visits to L1 from L2, i.e., $V_{B1F,T}$, which is the denominator in eq 5. We find that $V_{B1F,T}$ = 7020.

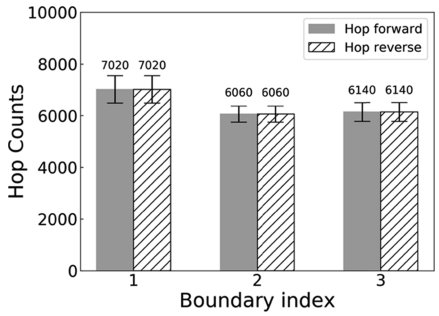

Figure 5. The number of times the methanol molecule crosses boundaries B1−B3 in the forward (solid) and reverse (hashed) directions. The results represent the average of 10 simulation runs, and the error bars represents 95% confidence intervals.

4.2. Methanol Residence Time Distribution in Each Layer. Obtaining the numerator of eq 5 is more challenging. When the methanol molecule hops to a certain layer, it will stay there for some amount of time until hopping to another layer. The time between the two consecutive hops is the residence time for the individual directional hopping event. During the MD simulation, there will be multiple such hops, giving rise to a distribution of residence times. These are plotted for L1 (reverse direction) in Figure 6a and L2 (forward direction) in Figure 6b. Note that the residence times plotted in Figure 6 are not yet separated: they represent a sum of transitions. For example, if methanol has two possible SoS in L2, resulting in two diffusion rates (λ_1 and λ_2), then the data in Figure 6b are the sum of the distributions of these two SoS. To differentiate the different SoS in each layer, we fit an RSDF with a multi-exponential function to the residence time distributions for each layer

$$P(\tau > t) = \sum_{p=1}^{n} a_p e^{-\lambda_p t} \tag{6}$$

where a_p refers to the number of hopping events associated with that process. Some clarification is provided in the Supporting Information Section S8 about why λ_p is associated with a process rather than with an SoS.

For this work, the transition frequency λ_p is taken as the "rate" of hopping across a boundary layer in units of molecules per second. For first-order processes, the λ_p term is equal to the product of the concentration of methanol molecules in the layer and the effective rate constant for leaving the particular SoS, i.e., $\lambda_p = k^{eff}_{p,c}\, c_i = k^{eff}_{p,\eta}\, \eta_i$, where c_i is the absolute concentration of species i in a particular layer (e.g., in units of mol/L), $k^{eff}_{p,c}$ is the effective rate constant when expressed with

https://dx.doi.org/10.1021/acs.jctc.9b01249
J. Chem. Theory Comput. 2020, 16, 2680−2691

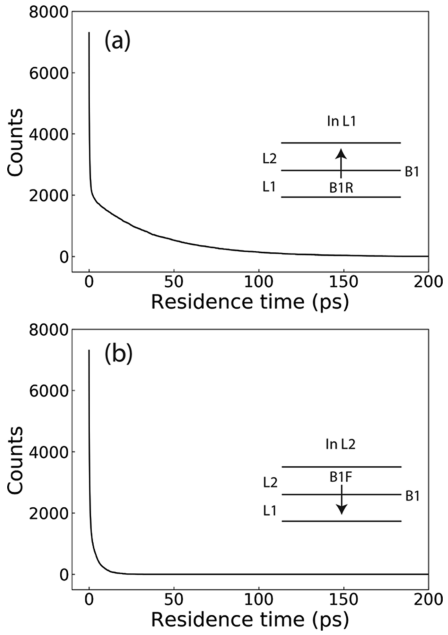

Figure 6. Raw Survival Distribution of methanol residence times for $\tau > t$ in (a) L1 and (b) L2. Each graph shows the count for discretized residence times in bins of 0.01 ps width. The counts in each graph encompass multiple SoS; data for the adsorbed SoS are encompassed within L1 (panel a). For clarity, only data from the first out of the 10 simulations are displayed.

absolute concentration units, and $k^{\mathrm{eff}}_{\mathrm{p},\eta}$ is the effective rate constant when expressed with relative concentration units. The relative concentration units used here are defined as follows: $\eta_i = \frac{c_i}{c_{\mathrm{single}}}$, where c_{single} corresponds to the concentration when there is one molecule contained within the volume associated with the layer. Thus, η_i is the number of molecules within that layer. The terms $k^{\mathrm{eff}}_{\mathrm{p},c}\, c_i$ and $k^{\mathrm{eff}}_{\mathrm{p},\eta}\, \eta_i$ are based on layer thickness (which in this work is = 3.7 Å) and thus have units that correspond to concentrations and process transition rates relative to the number of molecules in a layer of that specific thickness. The flux of molecules across a boundary (J_{B}) is given by $J_{\mathrm{B}} = \frac{k^{\mathrm{eff}}_{\mathrm{p},\eta}\, \eta_i}{\sigma_{\mathrm{B}}} = \frac{k^{\mathrm{eff}}_{\mathrm{p},c}\, c_i}{\sigma_{\mathrm{B}}}$, where σ_{B} is the area of the boundary. The simulated data in this work always correspond to a single molecule in a layer (because we never have more than one methanol in the system), and thus $\eta_i = 1$ for all transitions observed during simulations in this work, i.e., this work samples the special case where $\lambda_{\mathrm{p}} = k^{\mathrm{eff}}_{\mathrm{p},\eta} \times 1$ (though the method can be extended that is, to cases of arbitrary solute concentration). Since each SoS is inferred from a sampling of diffusion events that occur in various configurational environments, $k^{\mathrm{eff}}_{\mathrm{p},\eta}$ is an effective diffusion rate constant.

In fitting the raw survival distribution function to the data in Figure 6, we applied the simplest model capable of explaining the data. Hence, we initially assumed that each layer has only one SoS (so that n in eq 6 is equal to 1) and then we incrementally increased n until a good fit was obtained (see the Supporting Information for details). Comparing fits for n = 1, 2, and 3, we find that (i) n = 2 is sufficient to explain visits to L1 from L2 and (ii) visits from L1 to L2 (which include transitions from the adsorbed SoS) can be well described by n = 3. Results from fitting are tabulated in Table 1 and shown in Figure 7. Table 1 also includes the percentage of boundary

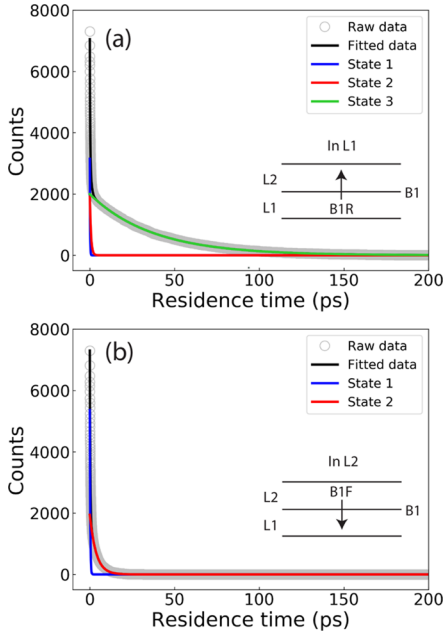

Figure 7. Fitted raw survival distribution functions (eq 6) of the residence times in (a) L1 and (b) L2. The fits shown have three B1-crossing processes in L1 and two B1-crossing processes in L2. For clarity, only data from the first out of the 10 simulations are displayed. Some of the raw data (gray circles) are obscured by the fitted functions.

crossings associated with each process (a_{p}%), which is calculated for process p by normalizing to a sum across all processes by $a_{\mathrm{p}}\% = a_{\mathrm{p}}/(\sum_{j=1}^{n} a_j)$.

In the interpretation presented here for the data in Table 1, the fitted values for λ_{p} reflect the rates of processes for leaving the associated layer. Furthermore, each λ_{p} is related to the effective diffusion and/or desorption rate for the process associated with leaving a specific non-adsorbed/adsorbed SoS. In L2, the λ_{p} values can only correspond to diffusion events and non-adsorbed SoS. It is interesting that even in L2, there are 2 types of diffusion processes, which could correspond to

Table 1. Parameters from Multi-Exponential Fitting of Residence Time Distributions Using Equation 6 for the Different Processes in L1 and L2[a]

	L1			L2		
process	a_{p}	a_{p}%	λ_{p} (ps^{-1})	a_{p}	a_{p}%	λ_{p} (ps^{-1})
1	3374 ± 254	48 ± 2.7	6.639 ± 0.448	5168 ± 404	74 ± 0.9	4.284 ± 0.08
2	1722 ± 232	25 ± 2.6	1.312 ± 0.132	1851 ± 115	26 ± 0.9	0.274 ± 0.01
3	1923 ± 157	27 ± 0.6	0.027 ± 0.001	N/A	N/A	N/A

[a]The results are the averages from 10 simulations at 300 K, and the +/− values are 95% confidence intervals.

https://dx.doi.org/10.1021/acs.jctc.9b01249
J. Chem. Theory Comput. 2020, 16, 2680−2691

the two different modes of diffusion for solutes in a solvent (i.e., as discussed by Nir and Stein[32]); however, our analysis does not enable us to discriminate between two processes of diffusion for a single type of solvated SoS versus two types of solvated SoS with separate diffusion processes (answering that question is saved for future work). For L1, two of the three λ_p values are on the same order of magnitude as those for L2. We ascribe these to diffusion processes. The third, which has a small value of 0.027 ± 0.001 ps^{-1}, we ascribe to surface adsorbed methanol. The observed value of $\lambda_{3,\,L1}$ = 0.027 reflects an average residence time due to three processes: (1) a molecule diffusing from the B1 boundary to the surface, (2) a molecule being adsorbed on a surface, and (3) a molecule diffusing from the surface back to the B1 boundary at the end of an adsorption visit. However, we know that the diffusion of non-adsorbed methanol occurs on a substantially faster time scale (as described by the much higher-hopping effective transition frequencies) and that the residence times in those diffusing SoS are negligible relative to the length of time spent in the adsorbed state. Consequently, the observed $\lambda_{3,\,L1}$ effective transition frequency is (by approximation) taken as the effective transition frequency for desorption. The associated occurrence of visits that include the adsorbed SoS, $V_{B1F,A}$, has a value of 1923 ± 157 (obtained from fitting as the coefficient a_p in eq 6).

4.3. Sticking Coefficient and Apparent Rate Constants. Inserting $V_{B1F,T}$ obtained in Section 4.1 with $V_{B1F,A}$ obtained in Section 4.2, we can use eq 6 to calculate the encounter sticking coefficient $S_E = \frac{V_{B1F,A}}{V_{B1F,T}} = 0.27$. Assuming an Arrhenius factor and conventional chemical kinetics theory, the sticking coefficient is related to the steric factor for the encounter sticking coefficient by $S_E = S_{E,0} \times e^{-E_{A,ads}/RT}$, where $S_{E,0}$ is the steric factor and $E_{A,ads}$ is the activation barrier for adsorption. The lower bound for $S_{E,0}$ (corresponding to the case where there is no adsorption barrier) is thus 0.27 at 300 K (the upper bound is by definition 1). While investigating the temperature dependence of adsorption and diffusion is beyond the scope of this work, application of the method presented here to obtain S_E at multiple temperatures would enable $S_{E,0}$ and $E_{A,ads}$ to be obtained.

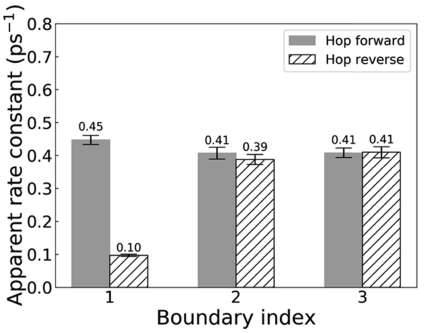

Figure 8. Apparent rate constant for methanol hopping crosses boundaries B1−B3 in the forward (solid) and reverse (hashed) directions. The error bars are the 95% confidence intervals.

The apparent rate constant for methanol hopping between layers, which is useful for kinetic modeling, is obtained in a similar manner to S_E. The apparent rate constant of methanol crossing a particular boundary encompasses the behavior of all SoS in that layer (as opposed to an effective rate constant, which is for a single SoS). The apparent rate constant of hopping can be obtained by

$$k^{app}_{O,B,D,\eta(hop)} = \frac{\text{number of visits that exited layer of origin O across boundary B in direction D}}{\text{total residence time in layer of origin O}} \quad (7)$$

For these rate constants, O is the layer number (associated with the layer of origin), B is the boundary plane being crossed, and D is the direction (either forward (F) or reverse (R)). The subscript η is as defined in Section 4.2. However, since the layer of origin can be inferred, we can simplify the notation, i.e., $k^{app}_{L2,\,B1,\,F,\,\eta(hop)}$ can be truncated to $k^{app}_{B1F,\,\eta(hop)}$. The total residence times for methanol in each layer and the maximum (longest) residence time for an individual visit are listed in Table 2. While no formal convergence or steady state analysis was performed,[40,41] it is evident that the simulation times were long enough for the values to have converged after averaging 10 runs.

Table 2. Total Residence Time of Methanol Spent in Each Layer and the Maximum Residence Time of a Single Visit in Each Layer[a]

layer	total residence time (ps)	percentage of total residence time during the whole MD simulation (%)	longest residence time observed for a single visit (ps)
1	73,040 ± 5760	36.5 ± 2.9	308 ± 31
2	15,617 ± 800	7.8 ± 0.4	35 ± 2
3	14,928 ± 488	7.5 ± 0.2	34 ± 2
4	15,090 ± 867	7.5 ± 0.4	33 ± 2

[a]The results represent the average of 10 simulation runs, and the error bars represents 95% confidence intervals.

Using eq 7 with values shown in Figure 4 (number of hops) and Table 2 (total residence time), the apparent rate constants for methanol hopping between layers are calculated and shown in Figure 8.

In Figure 8, it is interesting to compare $k^{app}_{B1F,\,\eta(hop)}$ (value of 0.45 × 10^{12} s^{-1}), which is the apparent rate constant of methanol hopping forward to the Pt surface from L2 to L1, and $k^{app}_{B1R,\,\eta(hop)}$ (value of 0.10 × 10^{12} s^{-1}), which is the apparent rate constant of methanol leaving the layer closest to the surface (L1). $k^{app}_{B1R,\,\eta(hop)}$ encompasses two kinds of hops: from visits where adsorption occurred *and* visits where adsorption did not occur. $k^{app}_{B1R,\,\eta(hop)}$ therefore does not reflect a single intrinsic rate constant. The ratio of $k^{app}_{B1F,\,\eta(hop)}/k^{app}_{B1R,\,\eta(hop)}$ displays the magnitude of difference in the kinetic residence times in the two layers. For this system, the residence time in L1 is dominated by the time in the adsorbed state, and thus $k^{app}_{B1F,\,\eta(hop)}/k^{app}_{B1R,\,\eta(hop)}$ is also an effective equilibrium constant for residing on the surface relative to solvation (this ratio directly compares the apparent rate constants of the hops between L1 and L2 and thus is free from any entropic effects from the size of the full solution space). This concept of an effective equilibrium constant is useful for relating the sticking coefficient to the bulk concentration, which is an exper-

https://dx.doi.org/10.1021/acs.jctc.9b01249
J. Chem. Theory Comput. 2020, 16, 2680−2691

imentally measurable quantity; tying this methodology to experimentally measurable quantities is further described below.

5. DISCUSSION

5.1. Extracting S_E and the Adsorption Rate Equation from Simulations. From the apparent rate constants, one can calculate the average flux and then obtain the expected adsorption rate using eq 1 ($r_{\text{ads},\sigma} = F_{1-s} \times S_E \times \theta_s$). The average flux is the same as the absolute rate per unit area and can be related to the hopping rate through $\langle F \rangle = r_{(\text{absl})} = r_{(\text{hop})} \times \frac{\text{molecules}}{\sigma_B}$, where the diamond brackets denote the arithmetic average and the word molecules is included as a unit conversion. In this study, the area of the layer boundary is also equal to the nominal surface area $\sigma_B = \sigma_S = 245.35\ \text{Å}^2$. Similar to the discussion in Section 4.2, $r_{(\text{hop})} = k^{\text{app}}_{c(\text{hop})} \times \langle c \rangle = k^{\text{app}}_{\eta(\text{hop})} \times \langle \eta \rangle$. From the above considerations, we are able to obtain the average flux into a layer L from across a particular boundary B by

$$\langle F_{L,B} \rangle = k^{\text{app}}_{O,B,D,c(\text{hop})} \times \langle c_O \rangle \times \frac{\text{molecules}}{\sigma_B} = k^{\text{app}}_{O,B,D,\eta(\text{hop})} \times \langle \eta_O \rangle \times \frac{\text{molecules}}{\sigma_B} \quad (8)$$

with subscripts as previously defined. Note that the left-hand side of eq 8 has a subscript L while the right-hand side has a subscript O: this is because we typically refer to the flux toward the surface, which depends on the concentration at the layer from which the molecules are entering. For adsorption to the surface, L is layer 1 and O is layer 2. Thus, as an example, when $\langle \eta_2 \rangle = 0.002$, the rate of adsorption on an empty surface would be given by

$$r_{\text{ads},\sigma} = F_{1-s} \times S_E \times \theta_s = \left(k^{\text{app}}_{L2,B1F,\eta(\text{hop})} \times \langle \eta_2 \rangle \times \frac{\text{molecules}}{\sigma_B} \right) \times S_E \times \theta_s = \left(0.45 \times 10^{12}\ s^{-1} \times 0.002 \times \frac{\text{molecules}}{245.35\ \text{Å}^2} \right) \times 0.27 \times 1$$

If desired, converting from $k^{\text{app}}_{O,B,D,\eta(\text{hop})}$ to $k^{\text{app}}_{O,B,D,c(\text{hop})}$ is accomplished using $k^{\text{app}}_{O,B,D,\eta(\text{hop})} \times {c_{\text{single}}}^{-1} = k^{\text{app}}_{O,B,D,c(\text{hop})}$, where c_{single} corresponds to the concentration for one molecule per volume associated with a layer, as discussed in Section 4.2. Then

$$r_{\text{ads},\sigma} = F_{1-s} \times S_E \times \theta_s = \left(k^{\text{app}}_{L2,B1F,c(\text{hop})} \times \langle c_2 \rangle \times \frac{\text{molecules}}{\sigma_B} \right) \times S_E \times \theta_s = \left(k^{\text{app}}_{L2,B1F,\eta(\text{hop})} \times {c_{\text{single}}}^{-1} \times \langle c_2 \rangle \times \frac{\text{molecules}}{\sigma_B} \right) \times S_E \times \theta_s$$

It is worth noting that even at equilibrium the concentration in L2 may be different from that deep in the bulk. For cases where there are no mass transfer limitations, it is convenient to use the equilibrium ratio of L2 relative to the bulk (in this present study, the concentration from L3 is a bulk concentration). The effective equilibrium constant is calculated by $K_{2b} = \langle c_b \rangle / \langle c_2 \rangle = \langle \eta_b \rangle / \langle \eta_2 \rangle$, where for this system, values of $\langle \eta_b \rangle$ and $\langle \eta_2 \rangle$ are from Table 2 with $\langle \eta_b \rangle = 0.075$ and $\langle \eta_2 \rangle = 0.078$, which gives $K_{2b} = 0.96$. Now, if we obtain $\langle c_b \rangle$, we can calculate $\langle c_2 \rangle$ and get the adsorption rate. Notice that $\langle c_b \rangle$ is the average bulk concentration and is the quantity that is typically controlled experimentally. Thus, this approach will enable a more direct comparison with experiment for situations where equilibrium is maintained between $\langle c_2 \rangle$ and $\langle c_b \rangle$. For cases where adsorption is mass-transfer limited, $\langle \eta_2 \rangle$ can be calculated using numerical evaluation of Fick's law, as in refs 12 and 27. In this work, we have considered a situation where the adsorption occurs with the solute concentration sufficiently close to the dilute limit that the adsorption rate would be expected to be linear with solute concentration. However, with increasing solute concentrations, the sticking coefficient and adsorption rate would exhibit solute concentration dependence. The method presented here can be extended to investigating the concentration dependence of the adsorption rate by running simulations with varying concentrations of solute.

The method presented here can be used to produce experimentally relevant rates as follows. Consider a situation for the system in this work where the bulk methanol concentration $\langle c_b \rangle$ is $8.26 \times 10^{-5}\ \frac{\text{molecule}}{\text{Å}^3}$ and $\theta_S = 0.5$ and conditions where the concentration in $\langle c_2 \rangle$ is determined by equilibrium rather than mass transport, then $\langle c_2 \rangle = \langle c_b \rangle / K_{2b} = 8.61 \times 10^{-5}\ \frac{\text{molecule}}{\text{Å}^3}$, and the rate of adsorption is

$$r_{\text{ads},\sigma} = F_{1-s} \times S_E \times \theta_s = \left(k^{\text{app}}_{L2,B1F,\eta(\text{hop})} \times {c_{\text{single}}}^{-1} \times \langle c_2 \rangle \times \frac{\text{molecules}}{\sigma_B} \right) \times S_E \times \theta_s = \left(0.45 \times 10^{12}\ \text{s}^{-1} \times \left(\frac{1\ \text{molecule}}{907.80\ \text{Å}^3} \right)^{-1} \times 8.61 \times 10^{-5}\ \frac{\text{molecule}}{\text{Å}^3} \times \frac{\text{molecules}}{245.3 * \text{Å}^2} \right) \times 0.27 \times 0.5$$
$$= 1.94 \times 10^7 \text{molecules} \cdot \text{Å}^{-2} \cdot \text{s}^{-1} = 3.2 \times 10^3\ \text{mol} \cdot \text{m}^{-2} \cdot \text{s}^{-1}$$

which is in experimentally relevant units. We note, however, that the chemistry and rates are influenced by the methanol–Pt(111) interaction energy, which depends on the force field that is employed. The force field employed here captures physisorption but not chemisorption. Our DFT calculations (see ref 5 and the Supporting Information) indicate that the methanol molecule chemisorbs to Pt(111), and we recognize that the example in this paper is lacking that chemistry. Obtaining values that match experiment thus requires accurate force fields to capture the interaction between the methanol molecule and the Pt surface. This is a subject of ongoing work by our group and others.[42] The method described herein will accommodate the more chemically accurate force fields being developed, enabling one to obtain a sticking coefficient from simulation and subsequently an adsorption rate equation that relies only on bulk concentrations and the fraction of surface sites available.

The above rate equation can be used in microkinetic modeling and kinetic Monte Carlo simulations.[3] Additionally, as the bulk concentration is an easily controllable and measurable experimental quantity, the rate equation can also be used in conjunction with experimental studies, demonstrating the robust utility of the method. Furthermore, the method provides an improvement in physical realism relative to basing liquid–solid adsorption rates on the gas-phase partial pressure

https://dx.doi.org/10.1021/acs.jctc.9b01249
J. Chem. Theory Comput. 2020, 16, 2680–2691

(allowing greater accuracy in future elementary step kinetic modeling, such as in refs 43 and 44). A comparison of values from the method presented herein to those from algebraic approximations is provided in Section 5.2.

5.2. Estimating Steady-State Adsorption Rates for Non-simulated Systems. In the best case, the factors $k^{app}_{L2,B1F,\eta(hop)} \times {c_{single}}^{-1} \times \langle c_2 \rangle$ and K_{2b} are known, enabling the calculation of the rate of adsorption for arbitrary conditions by eq 8. However, it is worth considering what approximations can be used to estimate the rate of adsorption under steady state for non-simulated systems. The general case is that the rate of adsorption is given by the sticking coefficient, the flux (encounter frequency), and the percentage of surface that is unoccupied: $r_{ads,\sigma} = F_{l-s} \times S_E \times \theta_s$. Based on the simulations in this work, we are able to compare our results to algebraic approximations for the rate of adsorption for non-simulated systems. The flux is dependent on the solute concentration in layer 2. It is possible to employ approximations for the flux and set S_E and K_{2b} to 1, in which case the rate of adsorption can be approximated as a function of the bulk concentration, $r_{ads,\sigma} = f(c_b) \times \theta_s$. Additional discussion and the origins of the approximations below are provided in the Supporting Information Section S11.

One simple method would be to estimate the flux from layer 2 as being similar to that given by the mean displacement of the bulk diffusion coefficient, which we will denote with a subscript *bdc*,

$$r_{ads,\sigma,bdc} \sim \frac{D_b}{d^2} \times S_0 \times (e^{-E_{A,ads}/RT}) \times \theta_s \times \langle c_b \rangle \times (K_{2b})^{-1} \times d \quad (9)$$

where D_b is the bulk diffusion coefficient for the solute, S_0 is the steric factor from collision theory (in our notation, S_0 is just one term in the sticking coefficient), $E_{A,ads}$ is the activation energy for adsorption, θ_s is the fraction of empty sites, and d is the layer thickness, which is equal to the diameter of the solute molecule. As noted in the literature, for most liquid−solid catalytic reactions, the rate of adsorption does not have a high degree of rate control.[43] Thus, it is likely that for cases in which a reactant starts in the gas phase and then undergoes a solid-catalyzed reaction in the liquid phase, that there will often be a pre-equilibrium established between the gas phase and the solute. In this case, the term in eq 9 can be obtained by $\langle c_b \rangle = P_A \times (K^{pc}_H)^{-1}$, where the term K^{pc}_H is a Henry's law constant (used to obtain the equilibrium absolute concentration from the gas-phase partial pressure of the solute/adsorbate).[45] There are various types of Henry's law constants, and the reader is directed to the reference provided for further information on the various units that are possible in Henry's law constants. For small molecules the diffusion coefficient in liquids is typically $\sim 1.0 \times 10^{-9}$ m^2 s^{-1} (for example, $D_b = 2.0 \times 10^{-9}$ m^2 s^{-1}for methanol[46]), and the rate can be even further approximated as

$$r_{ads,\sigma,bdc} \sim 1.0 \times 10^{-9}\ m^2\ s^{-1} \times \theta_s \times \langle c_b \rangle \times d \quad (10)$$

where $\langle c_b \rangle$ can again be calculated as noted above. Further details about these approximations are provided in the Supporting Information Section S11.

An alternative method is based on the kinetic gas flux (eq 2). When correcting the density difference between the liquid phase and the gas phase, this turns out to be a good approximation for the flux across a plane in the liquid phase (see also refs 12 and 27). We denote this approximation with the subscript *kgf*:

$$r_{ads,\sigma,kgf} \sim \frac{P_A}{\sqrt{2\pi m k_B T}} \times S_0 \times (e^{-E_{A,ads}/RT}) \times \theta_s \times x \times (K_{2b})^{-1} \left((1-x)\frac{\rho_{(solvent)}}{\rho_{A(g)}} + (x)\frac{\rho_{(solute)}}{\rho_{A(g)}} \right) \quad (11)$$

where x is the mole fraction of the solute in the solvent as obtained by $x = P_A(K^{px}_H)^{-1}$, $\rho_{(solvent)}$ is the molar density of the solvent in its pure bulk liquid form, $\rho_{(solute)}$ is the molar density of the solute in its pure bulk liquid form, and $\rho_{A(g)}$ is the density of the adsorbing species in the gas phase above the liquid. As liquids of small molecules are typically on the order of $\sim 10^3$ times more dense than gases at 1 bar, the equation can be further approximated for small molecules by

$$r_{ads,\sigma,kgf} \sim \frac{P}{\sqrt{2\pi m k_B T}} \times \theta_s \times x \times \left(10^3 \times \left(\frac{P_A}{1\ bar} \right)^{-1} \right) \quad (12)$$

where x can again be calculated as noted above.

The comparison of the values obtained by the various equations is shown in Table 3 for the methanol-to-Pt(111) adsorption rate simulated in this study for the case where T = 300 K, the bulk methanol-to-water concentration mole ratio is 1:150. Using a realistic value[45] of $(K^{pc}_H)^{-1} = 2.0$ mol m^{-3} Pa^{-1}, which corresponds to $K^{px}_H = 27.7 \times 10^3$ Pa, we see that this corresponds to a partial pressure of 184.4 Pa for methanol and gives a bulk molar concentration of $\langle c_b \rangle \sim 2.22 \times 10^{-4}$ methanol Å^{-3}. We see that eqs 9−12 provide reasonable order of magnitude estimates for the adsorption rate simulated in this study. Thus, the above algebraic expressions seem to provide a good intermediate term approximation for order of magnitude accuracy, which can be used in microkinetic modeling (elementary step kinetic modeling) of catalytic systems when constants from the methodology presented in this work are not available. In the long term, systematic studies based on the methodology presented in this study could result

Table 3. Comparison of Estimates for Steady-State Adsorption Rates[a]

equation	method for solute-to-surface flux estimation	estimated adsorption rate (molecules·m^2·s^{-1})	factor relative to equation 8
8	**extracted from MD**	**3.85×10^{28}**	**1.0**
2	kinetic gas flux directly	4.96×10^{24}	1.29×10^{-4}
9	bulk diffusion coefficient	1.20×10^{27}	3.12×10^{-2}
10	bulk diffusion coefficient further approximated	6.00×10^{26}	1.56×10^{-2}
11	kinetic gas flux with density correction	2.47×10^{28}	6.41×10^{-1}
12	kinetic gas flux with density correction further approximated	1.82×10^{28}	4.71×10^{-1}

[a]The value obtained from the method presented herein is presented in bold. For eq 8, the constants from the simulations were utilized. For eqs 9−12, it was assumed that in the absence of simulations, the value of K_{2b} would be unknown. Thus, for eqs 9−12, the values used were $K_{2b} = 1$, $d = 3.7$ Å, $K^{px}_H = 0.273$ atm, and $(K^{pc}_H)^{-1} = 2.0$ mol m^{-3} Pa^{-1}. For eq 10, a D_b of 2.0×10^{-9} m^2 s^{-1} was used. For eqs 9 and 11, $S_0 \times (e^{-E_{A,ads}/RT}) = 1$ was used. For all cases, $\theta_s = 1.0$ was used.

https://dx.doi.org/10.1021/acs.jctc.9b01249
J. Chem. Theory Comput. 2020, 16, 2680−2691

Table A1. Terminology Used for Deriving Sticking Coefficient at Liquid−Solid Interface, Listed in Alphabetic Order

term/variable	definition
adjacent layer	the volumetric cross section of solution that is within 1 molecular diameter of the surface (e.g., L1 in Figure 2)
bulk layer	volumetric cross sections of solution that are 1 molecular diameter wide and not adjacent to the Pt surface (e.g., L3 in Figure 2)
boundary	planes used to distinguish neighboring layers. (e.g., B1 represents the boundary between L1 and L2 in Figure 2)
collision	A *collision* occurs when the distance between the center of a molecule and the nucleus of a surface atom is less than or equal to the sum of their radii (see Figure 1 and the Supporting Information).
encounter	An *encounter* occurs when the distance between the center of a molecule and the edge of a surface atom is less than or equal to the kinetic diameter of the molecule (see Figure 1 and the Supporting Information).
layer	a volume cross section (or voxel) of the solution with height equal to the diameter of the methanol molecule.
process	A *process* is a kinetically distinct type of transition between states or lumped states. Examples include diffusion between layers in this work, desorption, or a chemical reaction.
sticking	*Sticking* occurs when a molecule stays on the surface in a defined adsorption state and can be entered directly from a *collision* or via a precursor state such as by *trapping*.
trapping	*Trapping* occurs when a molecule enters a short-lived adsorbed state (up to microseconds) following a collision, without being confined to a discrete surface site.
visits (number of visits is denoted with variable V)	A *visit* occurs when a molecule hops into a layer for a finite amount of time. We use subscripts to track the history of a particular visit. For example, $V_{B1F,T}$ represents the total number (T) of visits originating from layer 2 to layer 1 (i.e., across boundary B1 in the forward direction (F)).
RSDF	raw survival distribution function: the complementary cumulative distribution function of the Poisson distribution based on raw input rather than the normalized probability. Further defined in the text.
S_E	*encounter sticking coefficient*: the probability per encounter that a molecule ends up sticking
S_C	*collision sticking coefficient*: the probability per collision that a molecule ends up sticking
SoS	*set of states*: A molecule (solute) can experience many conformations due to various possible solvation orientations: when there is no large chemical difference between these states, such states can be chemically/physically lumped into a single set of states (SoS). Thus, the states of a molecule in a layer can be approximated by a finite number of SoS (the example presented in this work employs 2−3 SoS).
τ	*residence time*: Here, generally used for the time that a molecule spends in a layer before hopping to the next layer. In this work, the directions are also tracked using subscripts: $\tau_{B1F,T}$ denotes the total residence time (T) that molecule spends in layer 2 before it hops to layer 1 (forward hopping (F) to the Pt surface via boundary B1).

in more accurate system specific approximations (for example, by machine learning).

6. CONCLUSIONS

In this work, we developed a method using molecular dynamics (MD) simulations to calculate the encounter sticking coefficient (S_E) and the adsorption rate for liquid-phase solutes adsorbing to a solid surface. The method was applied to the case of methanol adsorbing molecularly on a Pt(111) surface under aqueous conditions. The residence times of the molecule in the direction normal to the Pt(111) surface were fitted using Poisson distributions with the assumption that motions of the molecule can be coarse grained into consecutive hops based on their positions during MD simulations. Using this methodology, encounters of the methanol molecule with the Pt surface were quantified, and adsorbed and non-adsorbed states near the Pt(111) surface were discerned by fitting to a raw survival distribution function (RSDF). Our procedure provides a straightforward way to extract the encounter sticking coefficient in liquid−solid adsorption. After obtaining the sticking coefficient, a rate equation for adsorption related to the bulk concentrations can then be written. The rate equation allows this methodology to create inputs for microkinetic modeling and kinetic Monte Carlo simulations. Additionally, as the bulk concentration is an easily controllable and measurable experimental quantity, the apparent rate constant can also be used in conjunction with experimental studies. Application of this method should enable simulation-based screening studies, such as across different solvents, various concentrations, etc. Using insights from this study, we present several algebraic approximations that can be used for systems where molecular dynamics simulations are not explicitly carried out. Comparisons of the adsorption rates obtained from the algebraic expressions show that they can achieve order of magnitude accuracy for adsorption rates under equilibrium conditions and are suitable for kinetic modeling of catalytic systems.

APPENDIX A1

Terms and definitions are provided in Table A1.

ASSOCIATED CONTENT

Supporting Information

The Supporting Information is available free of charge at https://pubs.acs.org/doi/10.1021/acs.jctc.9b01249.

Calculation of kinetic diameter of the methanol molecule from density functional theory, molecular dynamics force field parameters, discussion about how layer heights and positions were determined and their influence on the sticking coefficient, details about the fitting procedure for the Poisson distribution, comparison of sticking probability calculation with other methods, and data from all 10 molecular dynamics (MD) simulations (PDF)

AUTHOR INFORMATION

Corresponding Authors

Aditya Savara − *Chemical Sciences Division, Oak Ridge National Laboratory, Oak Ridge, Tennessee 37831, United States;* orcid.org/0000-0002-1937-2571; Email: savaraa@ornl.gov

Rachel B. Getman − *Department of Chemical and Biomolecular Engineering, Clemson University, Clemson, South Carolina 29634-0909, United States;* orcid.org/0000-0003-0755-0534; Email: rgetman@clemson.edu

Author

Xiaohong Zhang − *Department of Chemical and Biomolecular Engineering, Clemson University, Clemson, South Carolina 29634-0909, United States*

https://dx.doi.org/10.1021/acs.jctc.9b01249
J. Chem. Theory Comput. 2020, 16, 2680−2691

Complete contact information is available at:
https://pubs.acs.org/10.1021/acs.jctc.9b01249

Notes

The authors declare no competing financial interest.

■ ACKNOWLEDGMENTS

Work by X.Z. and R.B.G. was funded by the National Science Foundation under grant no. CBET-1554385. Work by A.S. was supported by the U.S. Department of Energy, Office of Science, Basic Energy Sciences, Chemical Sciences, Geosciences, and Biosciences Division. All simulations were performed on the Palmetto Supercomputer Cluster, which is maintained by the Cyberinfrastructure Technology Integration Group at Clemson University. The authors thank Prof. Robert Lund from the Clemson University Department of Math Sciences for the helpful discussions and one of the peer reviewers of this manuscript for the suggestion to consider how the methodology presented herein could be related to values derived from Henry's law constants.

■ REFERENCES

(1) Davies, P. R. On the Role of Water in Heterogeneous Catalysis: A Tribute to Professor M. Wyn Roberts. *Top. Catal.* **2016**, *59*, 671−677.
(2) Zhang, X.; Sewell, T. E.; Glatz, B.; Sarupria, S.; Getman, R. B. On the water structure at hydrophobic interfaces and the roles of water on transition-metal catalyzed reactions: A short review. *Catal. Today* **2017**, *285*, 57−64.
(3) Matera, S.; Schneider, W. F.; Heyden, A.; Savara, A. Progress in Accurate Chemical Kinetic Modeling, Simulations, and Parameter Estimation for Heterogeneous Catalysis. *ACS Catal.* **2019**, *9*, 6624−6647.
(4) Hibbitts, D. D.; Loveless, B. T.; Neurock, M.; Iglesia, E. Mechanistic Role of Water on the Rate and Selectivity of Fischer-Tropsch Synthesis on Ruthenium Catalysts. *Angew. Chem., Int. Ed.* **2013**, *52*, 12273−12278.
(5) Bodenschatz, C. J.; Xie, T.; Zhang, X.; Getman, R. B. Insights into how the aqueous environment influences the kinetics and mechanisms of heterogeneously-catalyzed COH* and CH_3OH* dehydrogenation reactions on Pt(111). *Phys. Chem. Chem. Phys.* **2019**, *21*, 9895−9904.
(6) Zhang, X.; DeFever, R. S.; Sarupria, S.; Getman, R. B. Free Energies of Catalytic Species Adsorbed to Pt(111) Surfaces under Liquid Solvent Calculated Using Classical and Quantum Approaches. *J. Chem. Inf. Model.* **2019**, *59*, 2190−2198.
(7) Singh, N.; Campbell, C. T. A Simple Bond-Additivity Model Explains Large Decreases in Heats of Adsorption in Solvents Versus Gas Phase: A Case Study with Phenol on Pt(111) in Water. *ACS Catal.* **2019**, *9*, 8116−8127.
(8) Salvestrini, S. A modification of the Langmuir rate equation for diffusion-controlled adsorption kinetics. *React. Kinet., Mech. Catal.* **2019**, *128*, 571−586.
(9) Cortright, R. D.; Dumesic, J. A. Kinetics of heterogeneous catalytic reactions: Analysis of reaction schemes. *Adv. Catal.* **2001**, *46*, 161−264.
(10) Savara, A.; Rossetti, I.; Chan-Thaw, C. E.; Prati, L.; Villa, A. Microkinetic Modeling of Benzyl Alcohol Oxidation on Carbon-Supported Palladium Nanoparticles. *ChemCatChem* **2016**, *8*, 2482−2491.
(11) Chorkendorff, I. B.; Niemantsverdriet, J. W. *Concepts of modern catalysis and kinetics*; John Wiley & Sons, 2017.
(12) Jung, L. S.; Campbell, C. T. Sticking probabilities in adsorption of alkanethiols from liquid ethanol solution onto gold. *J. Phys. Chem. B* **2000**, *104*, 11168−11178.
(13) Chen, M. S.; White, M. C. Combined Effects on Selectivity in Fe-Catalyzed Methylene Oxidation. *Science* **2010**, *327*, 566−571.
(14) Vattuone, L.; Gerbi, A.; Rocca, M.; Valbusa, U.; Pirani, F.; Vecchiocattivi, F.; Cappelletti, D. Stereodynamic effects in the adsorption of ethylene onto a metal surface. *Angew. Chem., Int. Ed.* **2004**, *43*, 5200−5203.
(15) Muino, R. D.; Busnengo, H. F. *Dynamics of Gas-Surface Interactions: Atomic-level Understanding of Scattering Processes at Surfaces*; Springer Berlin Heidelberg, 2013.
(16) Kresse, G. Dissociation and sticking of H_2 On the Ni(111), (100), and (110) substrate. *Phys. Rev. B* **2000**, *62*, 8295−8305.
(17) Ludwig, J.; Vlachos, D. G. First principles modeling of dissociative adsorption at crystal surfaces: Hydrogen on Pt(111). *Mol. Simul.* **2004**, *30*, 765−771.
(18) Stampfl, C.; Kreuzer, H. J.; Payne, S. H.; Pfnür, H.; Scheffler, M. First-principles theory of surface thermodynamics and kinetics. *Phys. Rev. Lett.* **1999**, *83*, 2993−2996.
(19) Groß, A. Dynamics of molecule-surface interactions from first principles. *Chem. Phys. Solid Surf.* **2003**, *11*, 1−26.
(20) He, J.; Acharyya, K.; Vidali, G. Sticking of Molecules on Nonporous Amorphous Water Ice. *Astrophys. J.* **2016**, *823*, 56.
(21) Hoffmann, J.; Schauermann, S.; Johánek, V.; Hartmann, J.; Libuda, J. The kinetics of methanol oxidation on a supported Pd model catalyst: molecular beam and TR-IRAS experiments. *J. Catal.* **2003**, *213*, 176−190.
(22) Karakalos, S.; Lawton, T. J.; Lucci, F. R.; Sykes, E. C. H.; Zaera, F. Enantiospecific Kinetics in Surface Adsorption: Propylene Oxide on Pt(111) Surfaces. *J. Phys. Chem. C* **2013**, *117*, 18588−18594.
(23) Kleyn, A. W. Molecular beams and chemical dynamics at surfaces. *Chem. Soc. Rev.* **2003**, *32*, 87−95.
(24) Österlund, L.; Zoric-Acute, I.; Kasemo, B. Dissociative sticking of O_2 on Al(111). *Phys. Rev. B* **1997**, *55*, 15452−15455.
(25) Panczyk, T. Sticking coefficient and pressure dependence of desorption rate in the statistical rate theory approach to the kinetics of gas adsorption. Carbon monoxide adsorption/desorption rates on the polycrystalline rhodium surface. *Phys. Chem. Chem. Phys.* **2006**, *8*, 3782−3795.
(26) Schweke, D.; Zalkind, S.; Attia, S.; Bloch, J. The Interaction of CO_2 with CeO_2 Powder Explored by Correlating Adsorption and Thermal Desorption Analyses. *J. Phys. Chem. C* **2018**, *122*, 9947−9957.
(27) Jung, L. S.; Campbell, C. T. Sticking probabilities in adsorption from liquid solutions: Alkylthiols on gold. *Phys. Rev. Lett.* **2000**, *84*, 5164−5167.
(28) Zhou, Y. G.; Stuart, E. J. E.; Pillay, J.; Vilakazi, S.; Tshikhudo, R.; Rees, N. V.; Compton, R. G. Electrode-nanoparticle collisions: The measurement of the sticking coefficients of gold and nickel nanoparticles from aqueous solution onto a carbon electrode. *Chem. Phys. Lett.* **2012**, *551*, 68−71.
(29) Wang, D.; Wu, H.; Schwartz, D. K. Three-Dimensional Tracking of Interfacial Hopping Diffusion. *Phys. Rev. Lett.* **2017**, *119*, 268001.
(30) Weaver, D. R.; Pitt, W. G. Sticking Coefficients of Adsorbing Proteins. *Biomaterials* **1992**, *13*, 577−584.
(31) Apostolopoulou, M.; Santos, M. S.; Hamza, M.; Bui, T.; Economou, I. G.; Stamatakis, M.; Striolo, A. Quantifying Pore Width Effects on Diffusivity via a Novel 3D Stochastic Approach with Input

from Atomistic Molecular Dynamics Simulations. *J. Chem. Theory Comput.* **2019**, *15*, 6907−6922.
(32) Nir, S.; Stein, W. D. Two Modes of Diffusion in Liquids. *J. Chem. Phys.* **1971**, *55*, 1598−1603.
(33) Wang, B.; Kuo, J.; Bae, S. C.; Granick, S. When Brownian diffusion is not Gaussian. *Nat. Mater.* **2012**, *11*, 481−485.
(34) Montroll, E. W.; Weiss, G. H. Random Walks on Lattices. II. *J. Math. Phys.* **1965**, *6*, 167−181.
(35) Hartenstein, B.; Bässler, H.; Jakobs, A.; Kehr, K. W. Comparison between multiple trapping and multiple hopping transport in a random medium. *Phys. Rev. B* **1996**, *54*, 8574−8579.
(36) Bodenschatz, C. J.; Zhang, X.; Xie, T.; Arvay, J.; Sarupria, S.; Getman, R. B. Multiscale Sampling of a Heterogeneous Water/Metal Catalyst Interface using Density Functional Theory and Force-Field Molecular Dynamics. *J. Visualized Exp.* **2019**, No. e59284.
(37) MacKerell, A. D., Jr.; Bashford, D.; Bellott, M.; Dunbrack, R. L., Jr.; Evanseck, J. D.; Field, M. J.; Fischer, S.; Gao, J.; Guo, H.; Ha, S.; Joseph-McCarthy, D.; Kuchnir, L.; Kuczera, K.; Lau, F. T. K.; Mattos, C.; Michnick, S.; Ngo, T.; Nguyen, D. T.; Prodhom, B.; Reiher, W. E.; Roux, B.; Schlenkrich, M.; Smith, J. C.; Stote, R.; Straub, J.; Watanabe, M.; Wiórkiewicz-Kuczera, J.; Yin, D.; Karplus, M. All-atom empirical potential for molecular modeling and dynamics studies of proteins. *J. Phys. Chem. B* **1998**, *102*, 3586−3616.
(38) Kahn, K.; Bruice, T. C. Parameterization of OPLS-AA force field for the conformational analysis of macrocyclic polyketides. *J. Comput. Chem.* **2002**, *23*, 977−996.
(39) Rappe, A. K.; Casewit, C. J.; Colwell, K. S.; Goddard, W. A.; Skiff, W. M. Uff, a Full Periodic Table Force Field for Molecular Mechanics and Molecular Dynamics Simulations. *J. Am. Chem. Soc.* **1992**, *114*, 10024−10035.
(40) Nellis, C.; Danielson, T.; Savara, A.; Hin, C. The F-t-Pj-RG method: An adjacent-rolling-windows based steady-state detection technique for application to kinetic Monte Carlo simulations. *Comput. Phys. Commun.* **2018**, *232*, 124−138.
(41) Nellis, C.; Hin, C.; Savara, A. The φ-relation and a simple method to predict how many data points are needed for relevant steady-state detection. *AIChE J.* **2018**, *64*, 3354−3359.
(42) Steinmann, S. N.; Ferreira De Morais, R.; Götz, A. W.; Fleurat-Lessard, P.; Iannuzzi, M.; Sautet, P.; Michel, C. Force Field for Water over Pt(111): Development, Assessment, and Comparison. *J. Chem. Theory Comput.* **2018**, *14*, 3238−3251.
(43) Behtash, S.; Lu, J.; Walker, E.; Mamun, O.; Heyden, A. Solvent effects in the liquid phase hydrodeoxygenation of methyl propionate over a Pd(1 1 1) catalyst model. *J. Catal.* **2016**, *333*, 171−183.
(44) Mamun, O.; Walker, E.; Faheem, M.; Bond, J. Q.; Heyden, A. Theoretical Investigation of the Hydrodeoxygenation of Levulinic Acid to γ-Valerolactone over Ru(0001). *ACS Catal.* **2017**, *7*, 215−228.
(45) Sander, R. Compilation of Henry's law constants (version 4.0) for water as solvent. *Atmos. Chem. Phys.* **2015**, *15*, 4399−4981.
(46) Derlacki, Z. J.; Easteal, A. J.; Edge, A. V. J.; Woolf, L. A.; Roksandic, Z. Diffusion coefficients of methanol and water and the mutual diffusion coefficient in methanol-water solutions at 278 and 298 K. *J. Phys. Chem.* **1985**, *89*, 5318−5322.

https://dx.doi.org/10.1021/acs.jctc.9b01249
J. Chem. Theory Comput. 2020, 16, 2680−2691